Surface Evolution and Sediment Transport On Comet 67P/Churyumov-Gerasimenko. M. N. Barrington[1], S. P. D. Birch[2], A. Jindal[1], A. G. Hayes[1], P. Corlies[3], J.-B. Vincent[4]. [1]Cornell University, Ithaca, NY, [2]Massachussets Instituted of Technology, Cambridge, MA, [3]Spectral Sciences Inc., Burlington, MA, [4]DLR Institute of Planetary Research, Berlin, Germany

Introduction: Comets are composed of primitive materials that can provide clues to the formation of the early solar system. These materials have undergone unknown amounts of processing after migrating from their initial distant reservoirs to their current orbits [1]. Given their relatively shorter orbits and close perihelion passages, Jupiter Family Comets (JFCs) are particularly attractive for exploration. Several missions have visited JFCs, providing a wealth of information on the global structure and composition of comets, and revealing the presence of large regions of unconsolidated materials called 'smooth terrains' [2], [3], [4], [5], [6], [7]. Still, these missions only provided snapshots in time of activity on the surface, while the processes acting to shape these smooth terrains remained elusive. From 2014-2016, European Space Agency's (ESA's) Rosetta mission accompanied comet 67P-Churyumov-Gerasimenko (67P) before, during and after its perihelion approach in August of 2015 [7]. Rosetta's Optical, Spectroscopic, Infrared Remote Imaging System (OSIRIS) provided over 8,200 Near Angle Camera (NAC) images of the surface and coma, often collecting images multiple times a day over the span of its mission. Past observations [8] and models [9] have shown that there is a global transport of sediment originating from the southern heminucleus and following ballistic trajectories until landing in the north, but sediment transport within and between smooth terrains remains unexplored. The breadth of Rosetta's image data provide the spatial and temporal resolution necessary to see how comets surfaces, in particular smooth terrains, evolve. Herein we catalog meter to decameter scale changes in the smooth terrains of 67P to reveal and characterize sedimentary migration pathways across the comet.

Methods: We analyzed data from Rosetta's OSIRIS Near Angle Camera (NAC), which imaged 67P's surface and coma before, during, and after its 2015 perihelion. Using existing mapping **[**10], [11] and nomenclature [12**]**, we broke 67P's smooth terrains into 25 subregions to account for the complex geometry of the comet and Rosetta's viewing geometry and divided the two-year mission into three-month time bins. We selected reference images before perihelion (August 13, 2015) for each sub-region, and generated lists of images of each sub-region spanning from the date of the reference image to August 2016. We co-registered images to their respective reference image using ShapeViewer, a publicly available comet-viewing software (www.comet-toolbox.com) [13], and the ArcGIS software suite. We used ArcGIS to search for and annotate changes within each image. If we detected changes between two dates, we increased the cadence of image selection until no further images were available or no further changes were detected.

We classified changes into three categories: deposition, erosion, or redistribution of sediment, where redistribution indicates processes that change the locations of sediment within regions but are not clearly related to either deposition or erosion activity. Then we assigned the changes to their appropriate time bin based on the date they occurred.

Results: We draw four main conclusions from the spatial and temporal distribution of changes in 67P's smooth terrains:

i. Sediment is transported within and between regions. We frequently observed simultaneous erosion and deposition processes within a given region in the same time bin. Likewise, we observed that as one region undergoes erosion, lofted sediment appears to land in neighboring regions in the same time bin. For example, much of the sediment primarily eroded from subregions of Hapi in March-May 2015 appears to have deposited within Ma'at 2-4 in the same time frame, while some of the materials re-deposited in Hapi (Fig. 1).

ii. Erosion and Deposition follow the subsolar latitude and are influenced by local topography. Erosion activity is first observed in the neck, in Hapi 1in September 2014 then expands to the rest of the neck and internal regions by December 2014. We generally observe erosion and deposition at progressively lower latitudes until we see erosion activity within the southernmost smooth terrains of Khonsu in December 2015 and Imhotep 2 in January 2016, after the subsolar latitude reached its minimum and was rising northward once again.

iii. Scarp migration occurs mainly in equatorial and internal regions. Scarp front generation and migration appears to require two fundamental elements: topography and sufficient solar insolation. For this reason, both internal (neck and lobe-facing) regions exposed to re-radiation from either lobe and external equatorial regions whose polar summer occurs near perihelion exhibit the most scarp activity. Alternatively, we observe little to no scarp activity in the external mid-latitudes, which are in polar winter near perihelion.

iv. We observe net-zero erosion and deposition on top of either lobe, perhaps indicating the presence of terminal sediment sinks. We observed large areas of little to no activity within the mid-latitudes (~30-60° N) of both lobes. The timing of northern polar winter near perihelion, combined with comet geometry and the difficulty of sediment delivery to these regions all contribute to the creation of possible terminal sinks on 67P.

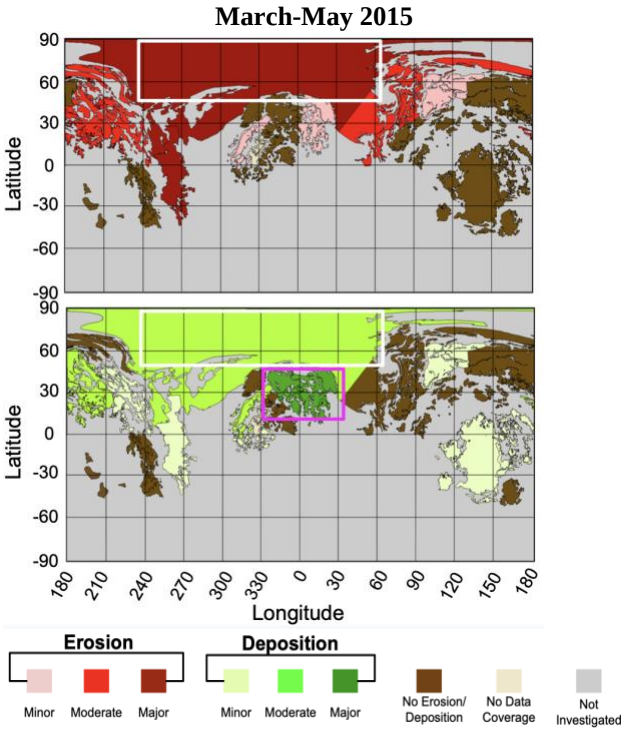

Fig. 1 – Top: Smooth terrain erosion from March-May 2015. Bottom: Smooth terrain deposition from the same time bin. Intraregional sediment erosion and deposition occurs in the Hapi 2 region (white box). Some of the same sediment eroded from Hapi 2 appears to have deposited within Ma'at 2-4 (magenta box).

Conclusions:

In addition to the transport of regolith from the consolidated southern heminucleus to the smooth terrains in the north, our observations suggest that sediment is locally transported within and amongst regions, often at the sub-kilometer scale. This erosion and deposition increased near perihelion and followed the subsolar latitude. The external mid-latitudes of 67P were most directly insolated near perihelion, which together with local topography drove scarp formation and migration. Likewise, regions scarp fronts formed in and near the neck due to reradiation from either lobe. However, since the tops of the lobes were in polar winter near perihelion, we observe very little net erosion or deposition within these regions, perhaps indicating both the difficulty of sediment delivery to these areas and the possibility that they behave as terminal sinks for such limited amounts of infalling sediment.

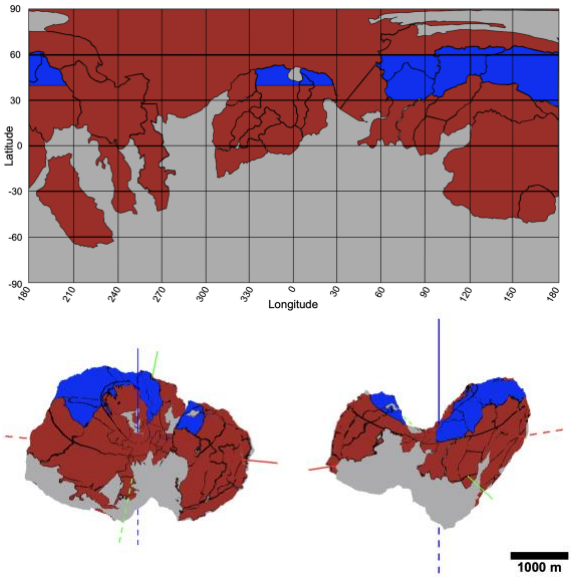

Fig. 2 – Regions of 67P's smooth terrains interpreted to act as terminal sinks are shown in blue, and erosionally active regions are shown in red in an equirectangular projection (top) and on three-dimensional models shown from two angles (bottom). The z-axis is shown in blue, x-axis is shown in red, and y-axis is shown in green. Negative axes are indicated by dotted lines.

Acknowledgments: This research was performed using publicly available data from the ESA's Archive Image Browser (https://imagearchives.esac.esa.int), and was partially funded by a Rosetta Data Analysis Program grant #80NSSC19K1307 and by the Heising-Simons Foundation (51 Pegasi b Fellowship to S.B.) We would also like to acknowledge Björn Davidsson, who contributed valuable advice to this work.

References:

[1] A'Hearn, M. F. et al. (2012) *The Astrohpys. Journ.*, *758*, 29–36. [2] Brownlee, D. E. (2004) *Science*, 304(5678), 1764-1769. [3] Thomas, P. C. (2013a) *Icarus*, 222(2), 453–466. [4] Veverka, J. et al. (2013) *Icarus*, 222(2), 424-435. [5] Thomas, P. C. (2013) *Icarus*, 222(2), 550-558. [6] El-Maarry, M. R. et al. (2017) *Science*, 355(6332), 1392-1395. [7] Keller, H. U. et al. (2007) *Space Sci. Rev.*, 128, 433-506. [8] Agarwal, J. (2010) *Icarus*, 207(2), 992-1012. [9] Keller, H. U. et al. (2017) *MNRAS*, 469(Suppl_2), S357-S371. [10] El-Maarry, M. R. et al. (2015) *Astron. & Astrophys.*, 583, A26. [11] Birch, S. P. D. et al. (2017) *MNRAS*, 469(Suppl_2), S50-S67. [12] Thomas, N. et al. (2015) *Science*, 347(6220), aaa0440. [13] Vincent, J.-B. et al. (2018) *LPSC XLIX*, Abstract #1281.